REFINEMENT OF THE CALIOP CLOUD MASK ALGORITHM

Shuichiro Katagiri[1]*, Kaori Sato[1], Kohei Ohta[1], Hajime Okamoto[1]
[1]*Research Institute for Applied Mechanics, Kyushu University, Kasuga, Kasuga koen 6-1, 816-8580, JAPAN, *Email: katagiri@riam.kyushu-u.ac.jp*

ABSTRACT

A modified cloud mask algorithm was applied to the CALIOP data to have more ability to detect the clouds in the lower atmosphere. In this algorithm, we also adopt the fully attenuation discrimination and the remain noise estimation using the data obtained at an altitude of 40 km to avoid contamination of stratospheric aerosols. The new cloud mask shows an increase in the lower cloud fraction. Comparison of the results to the data observed with a PML ground observation was also made.

1 INTRODUCTION

In the Earth climate system, clouds play a major role in the energy budget by means of atmospheric radiation processes [1] [2] and water cycles through distribution of rain on the ground [3], and besides transport water into the higher atmosphere. These important influences on the earth's climate are so complicated that a lot of observations cannot draw a convergent result. As for the atmospheric radiation, clouds have two competing effects: they partly reflect the solar radiation and therefore cool the atmosphere, while they partly interrupt the infrared radiation from the earth and thereby warm the atmosphere. The data sets of vertical cloud distribution are accordingly needed for the evaluation of the Earth climate system, especially for general circulation models (GCMs). Cesana *et al*. [4] evaluated cloud phase products from the Cloud-Aerosol Lidar and Infrared Pathfinder Satellite Observations (CALIPSO) [5] which include our product, and showed inconsistency among the products. Consequently, our algorithm using the CALIPSO data to make the cloud mask is to be refined. This algorithm is summarized in [6][7], and we improve it.

2 METHODOLOGY

We use the attenuated total backscattering coefficient β at 0.532 μm observed by the Cloud Aerosol Lidar with Orthogonal Polarization (CALIOP) onboard CALIPSO to discriminate the cloudy pixels. When the pixels with larger β than the threshold value β_{th} then the ones are recognized as the cloudy pixels. Mainly our algorithm is based on the threshold value β_{th} derived from the results of shipborne observations in the mid-latitudes [8] and in the tropical western Pacific [9] which is described as

$$\beta_{th}(z,R) = \frac{\beta_{th,aerosol} + \beta_{th,noise}(z,R)}{2} - \frac{\beta_{th,aerosol} - \beta_{th,noise}(z,R)}{2} tanh(z-5), \quad (1)$$

where

$$\beta_{th,aerosol} = 10^{-5.25}\ [1/m/sr], \quad (2)$$

and

$$\beta_{th,noise}(z,R) = \{P_m(z,R) + P_n + \sigma_n\}R^2 \quad (3)$$

where z and R denote altitude of the target pixel and the distance between CALIPSO and the surface of the earth, respectively, P_n and σ_n are the remain noises mean and standard deviation, respectively, after the calibration which is estimated with the data obtained from the high altitude to reduce the effects of clouds, aerosols, and polar stratospheric clouds (PSCs), and P_m is described as

$$P_m(z,r) = \beta_{mol}(z)/R^2. \quad (4)$$

Here $\beta_{mol}(z)$ is the volume molecular backscattering coefficient at an altitude of z calculated with the reanalysis data according to Hostetler *et al*. [10]. In this refinement of the algorithm, we changed the altitude where $\beta_{th,noise}$ is determined from 20 km to 40 km to avoid the stratospheric aerosol contamination. And if the pixels below the higher cloud layer have dominant signals, then the ones also are masked to be cloudy ones. In addition, we mask out the pixels on which the lidar signals are fully attenuated to discard undistinguishable pixels.

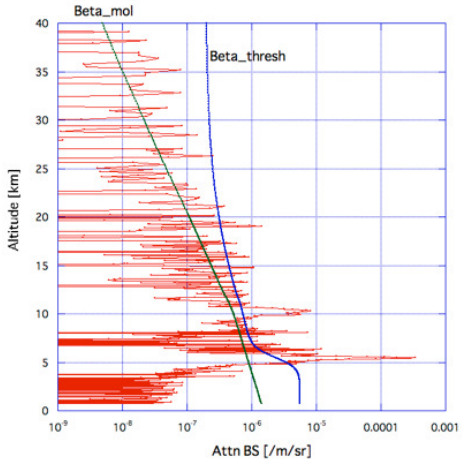

Figure 1 Example of the relationship, β (red line), β_{mol} (green) and β_{th} (blue).

Figure 1 illustrates the example of the raw data, which is the attenuated total backscattering coefficient β, received by CALIPSO (red lines), the calculated volume molecular backscattering coefficient β_{mol} (green), and the threshold value β_{th} (blue).

3 RESULTS

Figure 2 shows the raw signal β received by CALIOP (top panel) and the fully attenuated mask (bottom, blue colored) which is decided by referring to whether the surface return can be detectable or not. This fully attenuated mask roughly seems to be good, although sometimes noises near the surface disturb masking.

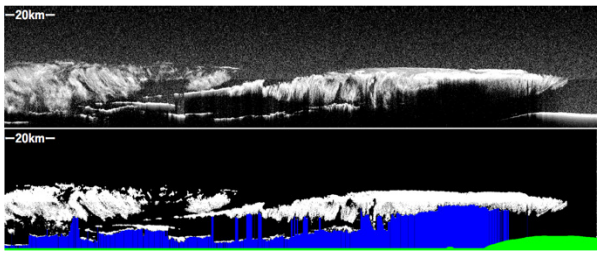

Figure 2 Fully attenuated mask (bottom, blue colored) and raw signal β (top)

The area colored blue is recognized as the fully attenuated pixels, therefore when the cloud fraction is estimated, they are not counted. Hence this improves the statistical cloud fraction. Figure 3 shows the cloud mask over Ny-Ålesund, Norway, where the left panel shows the original cloud mask which omits the detailed signals from clouds, the center panel shows the refined mask which deals with smaller signals than the original cloud mask, and the right panel shows the cloud mask using Micro pulse lidar observation from the ground. At this moment, there exists very optically thick low cloud below the higher cloud. These figures indicate that refined mask is extended around the top of the low optically thick cloud (below the red area in the center panel) compared to the original one, that is, the refined algorithm can mask deeper into the optically thick cloud than original one. The MPL laser beam cannot be transmitted through this thick low cloud, on the other hand, the laser beam from CALIPSO also is fully attenuated at the top of the cloud. Both lidar beam signals suggest the low cloud top is optically very thick, and therefore we should take into account the fully attenuated pixels in case that there is so optically thick cloud that the lidar cannot detect anything below the cloud.

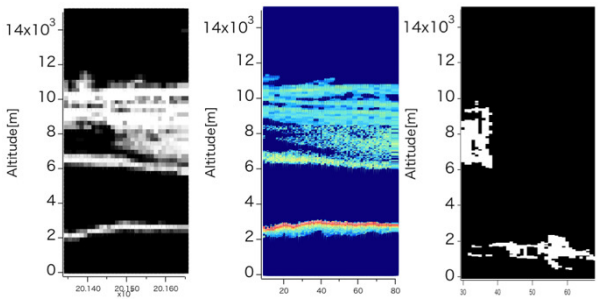

Figure 3 Cloud mask over Ny-Ålesund, original (left), refined (center), and Micro pulse lidar (MPL) (right)

Figure 4 shows the latitudinal cross section of the ice cloud fraction in January, 2009.

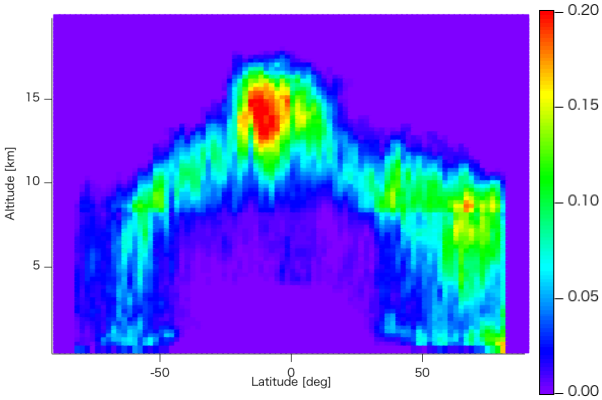

Figure 4 Cloud fraction (ice cloud)

Figure 5 shows the latitudinal cross section of the water cloud fraction. These two averaged cloud fractions have the vertical resolution of 240 m, and the horizontal resolution of 1.1 km. We use

the cloud phase discrimination algorithm made by Yoshida [11], which uses the relation between the depolarization ratio σ at 0.532 μm and the differential of attenuated backscattering coefficients *x'* at 0.532 μm to distinguish ice and water particles, where *x'* is defined as

$$x' = log_{10}\left[\frac{\partial\beta}{\partial z}\right] . \quad (5)$$

Water clouds generally have larger extinction coefficients than ice clouds at 0.532 μm, therefore the ratio of water clouds between *x'* and σ getting larger more slowly than ice clouds. This property is used in the cloud phase discrimination algorithm.

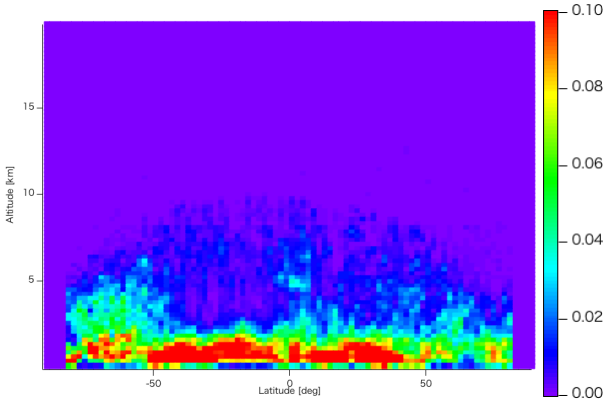

Figure 5 Cloud fraction (water cloud)

The refined algorithm result of the ice cloud mask is almost the same as the original one. However, the result of the water cloud takes slightly larger values than original algorithm. This indicate that the discrimination of the fully attenuated pixel is efficient for the statistical treatment of the lower clouds.

4 CONCLUSIONS

Our algorithm of the cloud mask was refined to have the fully attenuation discrimination, therefore there can be seen larger cloud fraction especially in the water cloud cases. This reduces the uncertainty of the statistical cloud fraction. The comparison to the ground observation by MPL indicates this refinement spread the ability of masking cloud pixels in lower optically thick clouds.

ACKNOWLEDGEMENTS

CALIPSO data were obtained from the Atmospheric Sciences Data Center at NASA's Langley Research Center. MPL is conducted by National Institute of Polar Research (NIPR). This study was supported by JSPS KAKENHI Grant Numbers JP17H06139, JP15K17762, JP25247078 and JP15K17762, by Green Network of Excellence (GRENE) Program Arctic Climate Change Project and the Arctic Challenge for Sustainability (ArCS), by the Japan Aerospace Exploration Agency for EarthCARE Research Announcement and by the Collaborative Research Program of Research Institute for Applied Mechanics, Kyushu University.

References

[1] Charlock, T. P., Ramanathan, V., 1985: The albedo field and cloud radiative forcing produced by a general circulation model with internally generated cloud optics, *J. Atmos. Sci.* **42**, 1408–1429.

[2] Ramanathan, V., Cess, R. D., Harrison, E. F., Minnis, P., Barkstrom, B. R., Ahmad, E., Hartmann, D., 1989: Cloud-radiative forcing and climate: Results from the Earth Radiation Budget Experiment, *Science* **243**, 57–63.

[3] Trenberth, K. E., Fasullo, J. T., Mackaro, J., 2011: Atmospheric moisture transports from ocean to land and global energy flows in reanalyses, *J. Climate* **24**, 4907–4924, doi:10.1175/2011JCLI4171.1.

[4] Cesana, G., Chepfer, H., Winker, D., Getzewich, B., Cai, X., Jourdan, O., Mioche, G., Okamoto, O., Hagihara, Y., Noel, V., Reverdy, M., 2016: Using in situ airborne measurements to evaluate three cloud phase products derived from CALIPSO, *J. Geophys. Res. Atmos.* **121**, 5788–5808, doi:10.1002/ 2015JD024334.

[5] Winker, D. M., Vaughan, M. A., Omar, A. H., Hu, Y., Powell, K. A., Liu, Z., Hunt, W. H., Young, S. A., 2009: Overview of the CALIPSO mission and CALIOP data processing algorithms, *J. Atmos. Oceanic Technol.* **26**, 2310–2323, doi:10.1175/2009JTECHA1281.1.

[6] Hagihara, Y., Okamoto, H., Yoshida R., 2010: Development of a combined CloudSat-CALIPSO cloud mask to show global cloud distribution, *J. Geophys. Res. Atmos.* **115**, D00H33, doi:10.1029/2009JD012344.

[7] Hagihara, Y., Okamoto, H., Luo, Z. J., 2014, Joint analysis of cloud top heights from CloudSat and CALIPSO: New insights into cloud top microphysics, *J. Geophys. Res. Atmos.* **119**, 4087–4106, doi:10.1002/2013JD020919.

[8] Okamoto, H., Nishizawa T., Takemura, T., Kumagai, H., Kuroiwa, H., Sugimoto, N., Matsui, I., Shimizu, A., Emori, S., Kamei, A., Nakajima, T., 2007: Vertical cloud structure observed from shipborne radar and lidar: Midlatitude case study during the MR01/K02 cruise of the research vessel Mirai, *J. Geophys. Res. Atmos.* **112**, D08216, doi:10.1029/2006JD007628.

[9] Okamoto, H., Nishizawa, T., Takemura, T., Sato, K., Kumagai, H., Ohno, Y., Sugimoto, N., Shimizu, A., Matsui, I., Nakajima, T., 2008, Vertical cloud properties in the tropical western Pacific Ocean: Validation of the CCSR/NIES/FRCGC GCM by shipborne radar and lidar, *J. Geophys. Res. Atmos.* **113**, D24213, doi:10.1029/2008JD009812.

[10] Hostetler, C. A., *et al*., 2006: CALIOP algorithm theoretical basis document, calibration and level 1 data products, Rep. PC-SCI-201, NASA Langley Res. Cent., Hampton, Va.

[11] Yoshida, R., Okamoto, H., Hagihara, Y., Ishimoto H., 2010, Global analysis of cloud phase and ice crystal orientation from Cloud-Aerosol Lidar and Infrared Pathfinder Satellite Observation (CALIPSO) data using attenuated backscattering and depolarization ratio, *J. Geophys. Res. Atmos.* **115**, D00H32, doi:10.1029/2009JD012334.